

Non-hydrodynamic modes from linear response in kinetic theory

Stephan Ochsenfeld^{1,*} and Sören Schlichting¹

¹Fakultät für Physik, Universität Bielefeld, Universitätsstrasse 25, D-33615 Bielefeld, Germany

Abstract. Viscous hydrodynamics serves as a successful mesoscopic description of the QGP produced in relativistic heavy-ion collisions. In order to investigate, how such an effective description emerges from the underlying microscopic dynamics we calculate the hydrodynamic and non-hydrodynamic modes of linear response in the sound channel from a first-principle calculation in kinetic theory. We do this with a new approach wherein we linearize and discretize the collision kernel to calculate eigenvalues directly. This allows us to study the Green's functions at any point in time or frequency space. Our study focuses on scalar theory with quartic interaction and we find that the analytic structure of Green's functions in the complex plane is far more complicated than just poles or cuts which is the first step towards an equivalent study in QCD kinetic theory.

1 Introduction

Understanding the Quark-Gluon-Plasma (QGP) created in Heavy-Ion Collisions (HICs) involves understanding its collective behavior. This is often done with the help of hydrodynamics which itself is a theory valid in the long time and long wavelength limit. Now the QGP is very short lived and the average system size is very small, raising questions about the applicability of hydrodynamics. Data collected from HIC experiments suggests that the space-time dynamics of the QGP can be indeed well modelled by hydrodynamic theories [1]. A relatively new way to look at the problem of (in)applicability of hydrodynamics is to analyze hydrodynamic and non-hydrodynamic modes [2, 3]. Naturally in a long time and long wavelength limit the system response to perturbation is purely hydrodynamic which can be seen in a Fourier picture in the form of hydrodynamic modes. Straying from this limit further and further one finds that additional modes become important in the system dynamics, those additional contributions are called non-hydrodynamic modes as they incorporate all the information that is not hydrodynamic. Understanding when the non-hydrodynamic modes dominate the system or when they become negligible can aid us in researching the bounds of applicability of hydrodynamics.

Kinetic theories are frequently used to describe the QGP as they capture both non-equilibrium behavior and converge towards hydrodynamics in the limit of long wavelengths [4, 5]. Because of these properties we will use kinetic theory to calculate both hydrodynamic and non-hydrodynamic modes in an ultra-relativistic conformal system and study their interplay at different gradient regimes. Details of this work can be found in [6].

*e-mail: s.ochsenfeld@uni-bielefeld.de

2 (Non)-Hydrodynamic Excitations in Kinetic Theory

Methodology. Starting point of our methodology in kinetic theory is the Boltzmann equation

$$p^\mu \partial_\mu f(\mathbf{p}, \mathbf{x}, t) = p C[f](\mathbf{p}, \mathbf{x}, t), \quad (1)$$

which describes the space-time evolution of the distribution function $f(\mathbf{p}, \mathbf{x}, t)$ with the collision integral C containing the microscopic information of the system. We will use a collision integral derived from scalar theory with quartic interaction (ϕ^4 theory) containing only elastic collisions in the form of $2 \leftrightarrow 2$ scatterings. The Boltzmann equation is linearized around an equilibrium background of ultra-relativistic massless bosons. The linear perturbations are then expressed as spatial Fourier modes with gradient strength $k = |\mathbf{k}|$ to receive

$$\left(\partial_t + i \frac{\mathbf{p}}{p} \cdot \mathbf{k}\right) \delta f_k(\mathbf{p}, t) = C[\delta f_k](\mathbf{p}, t). \quad (2)$$

In order to calculate eigenmodes of this equation we will expand the phase-space distribution into moments on a discretized grid of momenta and angles. In this form the Boltzmann equation becomes a simple vector matrix equation of the form $\partial_t \mathbf{N} = (C - K)\mathbf{N}$, with the discretized evolution matrix C and free-streaming matrix K as described in detail in [6].

We consider a small temperature (T) perturbation, that is localized in space, of the background equilibrium $\delta f_k(p, t = 0) = \delta T_0 \partial_T f_{eq}(p)$ as initial condition and then look at the energy response, also known as the sound channel. We then calculate the eigenvalues $\lambda_i(k)$ of this combined matrix $C - K$ to gather all the possible excitations of the system. By also calculating the eigenvectors of the evolution matrix we can decompose the system response completely into the individual (non-)hydrodynamic modes. The Green's function $G(t)$ describing the linear response of a macroscopic quantity to an initial perturbation, then we can write it as a sum of contributions of each mode

$$G(t) = \sum_i e^{\lambda_i t} \mu_i, \quad (3)$$

where μ_i are the weights of each mode, which depend on the quantity of interest and the initial condition. In this way we have a direct numerical way to compare modes and their impact on the system response. In particular, this simple analytical form can be easily translated into Fourier space, where each eigenvalue represents a simple pole in the complex frequency plane.

Scaling Variables. Since we study the spectrum of all possible excitations, it makes sense to first look at the hydrodynamic response, which will be useful for scale setting. In first order viscous hydrodynamics the energy response in the sound channel is given by

$$G(t) = \cos(c_s k t) e^{-\frac{2}{3} \frac{\eta}{sT} k^2 t} \quad (4)$$

with the speed of sound c_s and shear viscosity to entropy ratio η/s . One can see that this form is the result of two complex conjugated modes $\omega_\pm = \pm c_s k - i \frac{2}{3} \frac{\eta}{sT} k^2$. When expressed in terms of appropriate dimensionless scaling variables

$$\bar{k} = k \frac{\eta}{sT}, \quad \bar{t} = t \frac{sT}{\eta}, \quad \bar{\omega} = \omega \frac{\eta}{sT} \quad (5)$$

this response becomes universal across different microscopic theories [7], and we will use these scaling variables throughout our work.

(Non)-Hydrodynamic Excitations in ϕ^4 Theory. We present a compact summary of our results in Fig. 1, where various aspects of the system response in the sound channel

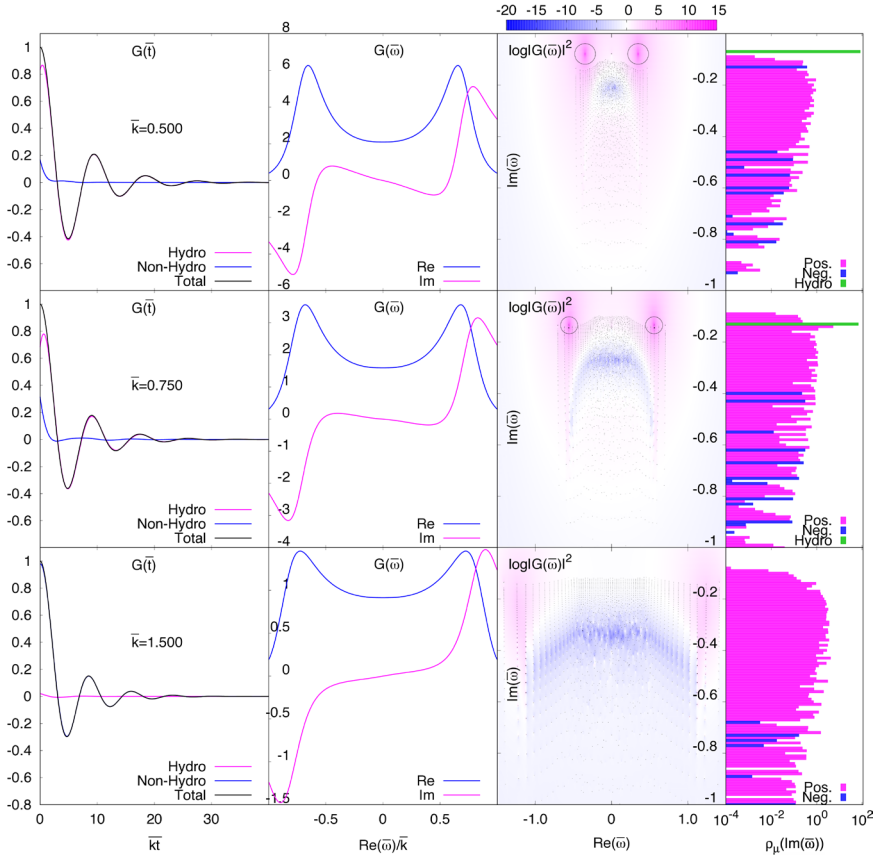


Figure 1. Left to right: 1. Green's function $G(\bar{t})$ decomposed into hydrodynamic and non-hydrodynamic contributions as function of $\bar{k}\bar{t}$. 2. Green's function $G(\bar{\omega})$ split into real and imaginary part as function of real frequency $\text{Re}(\bar{\omega})/\bar{k}$. 3. Eigenvalues of evolution operator as black circles in complex frequency plane, their sizes are scaled with their weights. Coloring in the plane is the logarithm of the absolute square of the Green's function $\log(|G(\bar{\omega})|^2)$ at that position in frequency space. 4. The weight density summed out over the real frequency range, the hydrodynamic mode weight is separate as green bar for comparison. Each row is for one gradient $\bar{k} = 0.5, 0.75, 1.5$ (top to bottom).

are presented for three different variations of \bar{k} . In our analysis we want to distinguish between hydrodynamic and non-hydrodynamic modes, which is non-trivial in a numerical calculation. We do this by assuming that the two eigenvalues with largest weight are the hydrodynamic ones. This description is valid until other non-hydrodynamic modes have weights comparable to the largest two. At this point we say that the hydrodynamic description breaks down, as it is clear that more than two modes significantly affect the dynamics.

Starting with the left most plots, the real time Green's functions, we find that for small gradients $\bar{k} = 0.5$ the evolution is almost purely hydrodynamic. Increasing \bar{k} shows that the non-hydrodynamic modes gain importance but the response is still dominated \bar{k} by hydrodynamic modes. Going to very high $\bar{k} = 1.5$ we see that the hydrodynamic response got completely overtaken by the non-hydrodynamic one. The next column of plots shows the Green's function in real frequency space. For small gradient strength we see two sharp peaks

in the real part and two steep inflection points in the imaginary part. The location of these corresponds with the location of the highest weight modes and their sharpness shows how close the modes are to the real axis. Increasing \bar{k} we see a smoothing of peaks and inflection points, showing that the hydrodynamic modes go deeper into the complex plane, gaining a stronger decay rate. For the highest \bar{k} the peaks have become flat. This tells us two things, either the strongest modes have gone very deep into the complex plane or a large region of modes gained in influence, for a rigorous conclusion we need the next column of plots. The third column of plots shows the eigenvalues in the complex frequency plane as black circles, with their size scaled by their weight, and the logarithm of the Green's function in the background color coding. For small \bar{k} there are two large distinct circles corresponding to the hydrodynamic modes. This shows that their contribution is the dominant one for this gradient strength. In the lower plane there are a few circles visible, showing that the non-hydrodynamic modes have a small, yet non-zero, influence in the response. By increasing \bar{k} we can see that the hydrodynamic modes gain larger decay rates, also the non-hydrodynamic region becomes larger and more visible, showing an increase of non-hydrodynamic contribution. For very large gradients the hydrodynamic modes vanished into the continuum of non-hydrodynamic modes. Here we can see that a wide region of modes, which is purely non-hydrodynamic, is responsible for the system dynamics. In the fourth column we can see a similar picture to the previous. The summed weights are showing clear dominance by hydrodynamics for small \bar{k} , with the green hydrodynamic contribution being several orders of magnitude larger than the rest. Increasing \bar{k} shows that the hydrodynamic modes are moving into the region of non-hydrodynamic ones. Their weight become smaller but they still stick out of non-hydrodynamic continuum. For large \bar{k} we see that no single mode is dominating the response and a whole region of non-zero weight is determining the dynamics instead.

3 Conclusion

We developed a new method to calculate non-hydrodynamic and hydrodynamic modes from a discretized Boltzmann equation. We studied the gradient dependence of modes in the sound channel for scalar ϕ^4 theory and found that the system dynamics are dominated by hydrodynamics for small gradients \bar{k} , while at large gradients the non-hydrodynamic modes take over this role. We can see that the hydrodynamic breakdown happens around a gradient scale of $\bar{k} \gtrsim 1$, but with a rather smooth transition instead of a rapid break. This gradient strength can be used to calculate a critical length scale $l_c \sim 1/k_c \approx 0.16 \text{ fm} \left(\frac{200 \text{ MeV}}{T}\right) \left(\frac{\eta/s}{0.16}\right)$ below which non-hydrodynamic modes dominate the dynamics.

Acknowledgement. This work is supported by the Deutsche Forschungsgemeinschaft (DFG) under grant CRC-TR 211 “Strong-interaction matter under extreme conditions” project no. 315477589-TRR 211. The authors gratefully acknowledge computing time provided by the Paderborn Center for Parallel Computing (PC2).

References

- [1] B.B. Abelev et al. (ALICE), *Phys. Rev. C* **90**, 054901 (2014), [1406.2474](#)
- [2] P. Romatschke, *Eur. Phys. J. C* **76**, 352 (2016), [1512.02641](#)
- [3] A. Kurkela, U.A. Wiedemann, *Eur. Phys. J. C* **79**, 776 (2019), [1712.04376](#)
- [4] P.B. Arnold, G.D. Moore, L.G. Yaffe, *JHEP* **01**, 030 (2003), [hep-ph/0209353](#)
- [5] A. Kurkela, A. Mazeliauskas, J.F. Paquet, S. Schlichting, D. Teaney, *Phys. Rev. Lett.* **122**, 122302 (2019), [1805.01604](#)
- [6] S. Ochsensfeld, S. Schlichting, *JHEP* **09**, 186 (2023), [2308.04491](#)
- [7] X. Du, S. Ochsensfeld, S. Schlichting (2023), [2306.09094](#)